Phase Morphologies and Mechanical Properties of High-Impact Polystyrene (HIPS) and Polycarbonate Blends Compatibilized with Polystyrene and Polyarylate Block Copolymer

HIROSHI OHISHI,[1], TAKAYUKI IKEHARA,[2] TOSHIO NISHI[2]

[1] Advanced Technology Research Laboratories, Nippon Steel Corporation, 20-1 Shintomi, Futtsu, Chiba, 293-8511, Japan

[2] Department of Applied Physics, School of Engineering, The University of Tokyo, 7-3-1 Hongo, Bunkyo-ku, Tokyo 113-8656, Japan

Received 30 December 1999; accepted 26 August 2000

ABSTRACT: Phase morphology and mechanical properties of blends of high-impact polystyrene (HIPS) and polycarbonate (PC) blends compatibilized with a polystyrene (PS) and polyarylate (PAr) (PS–PAr) block copolymer were investigated. Over a broad range of composition from 50/50 through 30/70, HIPS/PC blends formed cocontinuous structures induced by the flow during the extrusion or injection-molding processes. These cocontinuous phases had heterogeneity between the parallel and perpendicular directions to the flow. The micromorphology in the parallel direction to the flow consisted of stringlike phases, which were highly elongated along the flow. Their longitudinal size was long enough to be longer than 180 μm, while their lateral size was shorter than 5 μm, whereas that in the perpendicular direction to the flow showed a cocontinuous phase with regular spacing due to interconnection or blanching among the stringlike phases. The PS–PAr block copolymer was found to successfully compatibilize the HIPS/PC blends. The lateral size of the stringlike phases could be controlled both by the amount of the PS–PAr block copolymer added and by the shear rate during the extrusion or injection-molding process without changing their longitudinal size. The HIPS/PC blend compatibilized with 3 wt % of the PS–PAr block copolymer under an average shear rate of 675 s^{-1} showed a stringlike phase whose lateral size was reduced almost equal to the rubber particle size in HIPS. The tensile modulus and yield stress of the HIPS/PC blends could be explained by the addition rule of each component, while the elongation at break was almost equal to that of PC. These mechanical properties of the HIPS/PC blends can be explained by a parallel connection model independent of the HIPS and PC phases. On the other hand, the toughness factor of the HIPS/PC blends strongly depended on the lateral size of the stringlike phases and the rubber particle size in the HIPS. It was found that the size of the string phases and the rubber particle should be smaller than 1.0 μm to attain a reasonable energy absorbency by blending HIPS and PC. © 2001 John Wiley & Sons, Inc. J Appl Polym Sci 80: 2347–2360, 2001

Key words: high-impact polystyrene (HIPS); polycarbonate; polystyrene; polyarylate; block copolymer; *in situ* reaction; reactive processing; transesterification; compatibilizer; stringlike phase; flow-induced morphology

Correspondence to: H. Ohishi

Journal of Applied Polymer Science, Vol. 80, 2347–2360 (2001)

INTRODUCTION

Polymer blending is a simple and efficient method for designing and controlling the performance of polymeric materials using easily available polymers. Its procedure makes it possible to develop a new polymeric material of synergetic performance of each polymer, to reduce the cost of engineering plastics by diluting them with lower-cost polymers, or to enhance the recycling of spent plastics. These advantages of polymer blending on performance, economy, or ecology have accelerated R&D activities in the field of polymer blends or alloys in terms of academic and industrial interests.[1–5]

However, almost all simple polymer blends fail to compatibilize with each other due to their low combinatorial entropy of mixing. Owing to their poor interfacial adhesion strength, polymer blends among immiscible polymers usually lead to unsatisfactory properties by a simple mechanical mixing. Thus, improvement in the interfacial adhesion strength is a key factor for developing a new polymeric material by polymer blending.

A general concept for improvement in the interfacial adhesion strength between immiscible polymers was summarized in ref. 5. In the general industrialized compatibilization methods, addition of a block or graft copolymer is the most representive[6] and has been applied to several immiscible polymer systems.[5,7–11] A function of a block or graft copolymer has been shown to reduce the interfacial tension between two immiscible polymers[12] and to generate a finer dispersion during the processing,[13] leading to a dramatic increase in the interfacial adhesion strength.[14]

Although the addition of a block or graft copolymer appears to be effective, this method has a practical limitation for the following reason: When a block or graft copolymer is mixed with immiscible polymers, it often forms micelles by itself in either of the polymer phases instead of existing at the polymer–polymer interface.[15,16] Formation of micelles reduces the effectiveness of the block or graft copolymer as a compatibilizer significantly.[6] Another method is to add a polymer with functional groups which can generate a block or graft copolymer during blend preparation via an *in situ* interfacial reaction.[17–21] This approach, known as "reactive compatibilization," has been implemented in a number of commercial products in recent years.[5,17–23]

We carried out research and development on polymer blends based mainly on polystyrene and

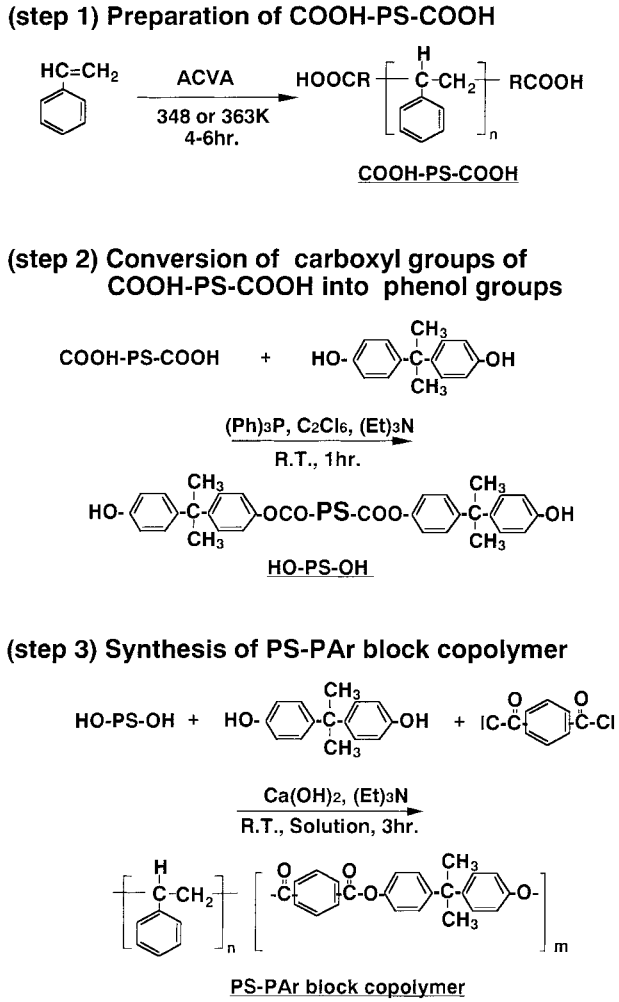

Figure 1 Reaction scheme for synthesis of PS–PAr block copolymer.

polyarylate (PS–PAr) block copolymers.[24–29] In our earlier publications, we proposed a novel synthetic procedure for a PS–PAr block copolymer (Fig. 1)[24–26] and reported its high potential for high-precision optical applications.[24,25,27]

In this research, we attempted to apply a PS–PAr block copolymer as a reactive compatibilizer for the immiscible blend system of high-impact polystyrene (HIPS) and polycarbonate (PC).[30–38] Unlike the case for polymer blends based on polyamides or polyesters, schemes for the formation of a block or graft polymer by an *in situ* reaction with PC are not popular. This is due mainly to the fact that terminal functional groups of the PC chain are usually capped for the prevention of the Fries transition. As a result, the terminal functional groups of the PC chain are not allowed to react with a reactive compatibilizer like poly-

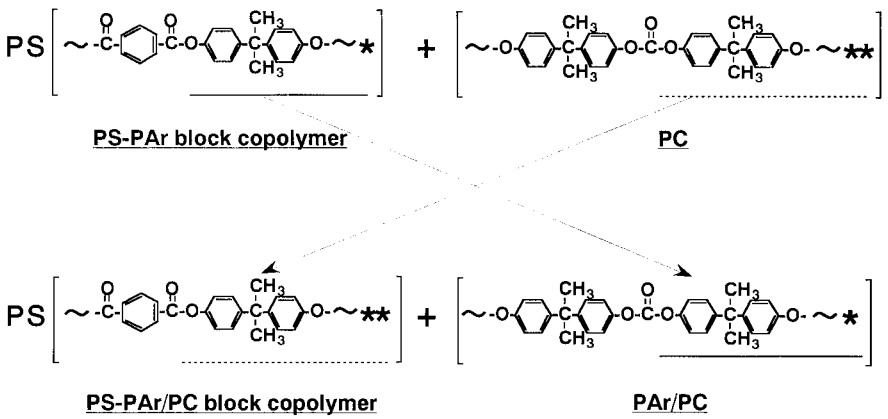

Figure 2 Transesterification between PS–PAr block copolymer and PC.

amides or polyesters. We paid attention to the experimental results that PAr chains in PS–PAr block copolymers were found to undergo transesterification[39] with PC during the extrusion process, even if PC is end-capped (Fig. 2).[29] Thus, by making use of the PAr and PS chains of the PS–PAr block copolymer as a reactive unit with PC and an anchor unit to the PS matrix of the HIPS phase, respectively, the PS–PAr block copolymer is expected to be applicable as a reactive compatibilizer for the HIPS and PC blend system.

The purpose of this article was to investigate the phase morphology of HIPS/PC blends compatibilized with the PS–PAr block copolymer and to discuss how the PS–PAr block copolymer is effective on the morphology generation. In addition, the relationship between the generated phase morphology and their mechanical properties was examined.

EXPERIMENTAL

Materials

The PS–PAr block copolymer was synthesized (Fig. 1) and characterized in the same way as described previously (Table I).[24,25] In this study, PAr weight percent in the PS–PAr block copolymer is defined by eq. (1) according to the same concept as described in ref. 29:

$$\text{PAr wt \%} = 10\,M_{\text{PAr}}/(M_{n_{\text{COOH—PS—COOH}}} + 10\,M_{\text{PAr}}) \quad (1)$$

where $Mn_{\text{COOH–PS–COOH}}$ and M_{PAr} are the number-average molecular weights of the fed COOH—PS—COOH in step 2 of Figure 1 and of the PAr unit, 358 g/mol, respectively. HIPS samples with different rubber particle size were obtained from the Nippon Steel Chemical Co. (Tokyo, Japan; XL-1 and H-650). The size of the rubber particle of XL-1and H-650 were 0.6 and 3.5 μm on average, respectively. XL-1 was used through all the experiments. H-650 was used only for the purpose of examining the effect of the rubber particle size on the impact strength of the HIPS/PC blends. PC was obtained from the Mitsubishi Chemical Corp. (Tokyo, Japan; Novarex 7025A), which was a general grade for injection molding. In the following, the blend composition is shown on a weight–composition basis.

Table I Preparation and Characterization of PS–PAr Block Copolymer

	COOH—PS—COOH			Feed Characterization of PS–PAr Block Copolymer				
Sample	M_n	M_W	COOH (equiv/mol)	PS/PAr	M_n[a]	M_W[a]	Homo-PAr[b] (wt %)	Block Copolymerization Ratio of PAr
PS–PAr block copolymer	20,000	39,000	2.01	85/15	32,000	85,000	0.5	96.7

[a] Number-average (M_n) and weight-average (M_W) molecular weight were measured without purification.
[b] Homo-PS and the pure PS–PAr block copolymer could not be devided due to limitation of the purification method.

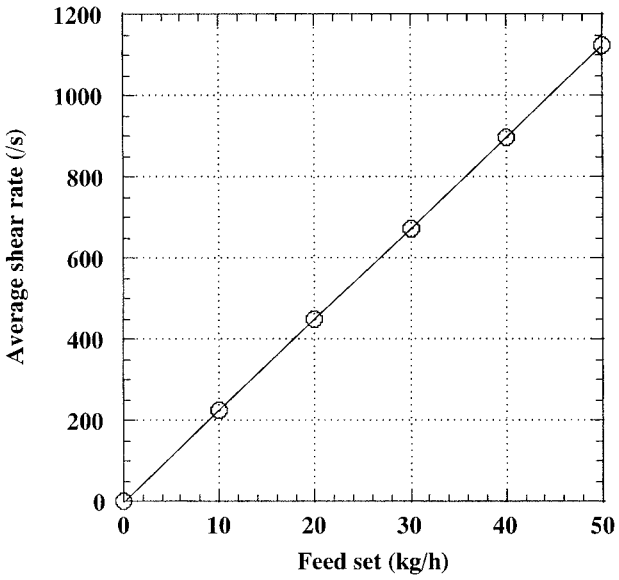

Figure 3 Feed set–average shear rate curve during the extrusion process.

Melt Processing

The blends of HIPS, PC, and the PS–PAr block copolymer were intensively melt-mixed by a corotating twin-screw extruder (Japan Steel Works Corp. Japan; TEX30SS, 30-mm diameter, L/D = 50, 120 rpm) at a feed rate of 30 kg/h under 260°C of barrel temperature. The average shear rate during the extrusion process was kept about 680 s^{-1} through all the experiments. For the purpose of examining the effect of the shear rate on the phase morphology, it varied from 225 to 900 s^{-1} by controlling the feed rate according to Figure 3. The extruded blends were pelletized and subsequently injection-molded under the condition of 260°C and 8000 kg cm^{-2} using an injection machine (Toyo Machinery Metal Corp., Japan; Ti-80G2) to prepare standard specimens for tensile strength and Izod-impact strength (1/8 in. in thickness) measurements. Before each processing experiment, all the polymeric materials were dried for at least 12 h at 90°C in a vacuum oven to ensure complete removal of the sorbed water.

Morphology Observation and Mechanical Properties Measurements

The blend morphologies were examined by a scanning electron microscope (SEM) or a transmission electron microscope (TEM). For SEM observation, the Izod or pelletized specimens were fractured in liquid nitrogen, followed by cyclohexane etching in an ultrasonic generator for 15 min to extract the HIPS phases. The etched specimens were washed several times by distilled water, followed by drying. The etched surface was coated with gold (30 nm in thickness). SEM observation was carried out using a Hitachi SEM, S-2100A at an accelerating voltage of 20 kV. In the SEM micrographs, darker portions were assigned to the HIPS-rich phases that were washed away by the etchant, while brighter portions were assigned to the PC-rich phases. For TEM observation, the microtomed specimens were first stained with osmium teroxide vapor for 1 day at room temperature to stain the rubber particle of polybutadiene (PB) in the HIPS phase selectively. Then, they were further stained by ruthenium teroxide vapor for 1 day at room temperature to obtain a clear contrast between the PS matrix in the HIPS and PC phase. TEM observation was carried out using a Hitachi TEM, H-7100FA at an accelerating voltage of 100 kV.

The tensile test was carried out according to ASTM D-638. Notched Izod impact strength was measured according to ASTM D-256 using a pendulum-type tester. At least 10 specimens were tested for each data point.

RESULTS AND DISCUSSION

Phase Morphologies of HIPS/PC Blends

Uncompatibilized HIPS/PC Blends

Figures 4(1,2) and 5 show the phase morphologies of the HIPS/PC blend at 50/50 and 30/70 compositions. The SEM micrographs in Figures 4(1,2) and 5 were obtained from a microsection of an Izod specimen in the parallel and perpendicular directions to the flow, respectively. At both compositions, they form a cocontinuous structure with heterogeneity between the parallel and perpendicular directions to the flow. For simplicity, the terms parallel and perpendicular to the flow are hereinafter referred to as the longitudinal and the lateral, respectively.

In the longitudinal morphology, both HIPS- and PC-rich phases are highly elongated along the flow direction as shown in Figure 4(1,2). The shape of these elongated phases looked like straight string undergoing several breakups, interconnections, and branchings. The stringlike phases oriented along the flow were long. They were at least longer than was the SEM scope of low magnification in Figure 4(1,2), which was

about 180 μm, while their lateral size was shorter than about 5 μm at both compositions. These highly elongated phases indicate that the concentration fluctuations parallel to the flow were much more suppressed by the flow than that normal to the flow. The two-dimensional fast Fourier transformation (2D-FFT) pattern analysis of the SEM micrographs in Figure 4(1,2) showed a sharp streak normal to the flow direction. They signify that these elongated phases have a high continuity and regularity in the parallel and normal directions to the flow, respectively. There was a difference in the stringlike phase size and area ratio of the darker phase between the 50/50 and 30/70 blends, although these differences between the core and skin parts were small. In the 30/70 blend, the lateral size of the stringlike phase was smaller than in the 50/50 blend. This could also be confirmed by the fact that the 2D-FFT analysis of the 30/70 blend showed a longer streak normal to the flow direction than that of the 50/50 blend. In addition, in the 30/70 blend, the area of the darker region was rather wider than that of the brighter region. This suggests that the PC-rich region should contain a large amount of HIPS in the 30/70 blend, while this tendency was not so clear in the 50/50 blend.

On the other hand, the micromorphology in the lateral section had a different appearance. Both the HIPS and PC phases appeared to form cocontinuous phases (Fig. 5) due to interconnection or blanching among the stringlike phases even at both compositions. There seemed little difference in their micromorphology between the core and skin parts, while there was a difference in the area ratio of the darker portion between the 50/50 and 30/70 blends as discussed above. In the 30/70 HIPS/PC blend, the area of the darker region seemed rather wider than that of the brighter region, indicating that the PC-rich region should contain significant amounts of HIPS. The size and periodicity of the cocontinuous phases are discussed in the next section because it was difficult to discuss these characteristics based only on the SEM micrographs in Figure 5.

These stringlike phases with such high orientation, continuity, and regularity as our experimental results could not be obtained by a simple mixing of immiscible polymer blend systems. These phenomena were reported to be observed in an immiscible polymer blend[40] or solution[41–46] system under a high shear rate condition near the homogenization point. Under such a high shear flow, two opposing factors are dominant for the generation of the phase morphology. One factor is the thermodynamic driving force, which causes composition fluctuation and promotes phase separation. The other factor is the hydrodynamic driving force which suppresses the growth of composition fluctuation or which elongates domains and eventually causes them to burst. A subtle balance between these two opposing factors forms the stringlike phase. Considering the process in blending HIPS and PC combined with the reported experimental results,[40–45] a mechanism for this kind of morphology generation could be postulated as follows: When the HIPS/PC blends were exposed to a high shear flow field of the aforementioned order during the extrusion or injection-molding process, the stringlike phases were formed. In the cooling stage, the melt blend was freed from this flow field. They were subject to further phase separation according to the phase diagram in the equilibrium state, that is, immiscible at the whole composition range,[30–38] until cooled down to the T_g of PC. As its cooling speed was faster than was the phase-separation kinetics, the stringlike phases were frozen in the molded blend by vitrification near the T_g.

HIPS/PC Blends Compatibilized with PS–PAr Block Copolymer

Figures 6 and 7 show how the morphology of 50/50 HIPS/PC blends was affected by the PS–PAr block copolymer. The amount of the added PS–PAr block copolymer was varied from 1 to 5 wt %. As the difference in size or shape of the stringlike phases between the skin and core parts was small, the SEM micrographs in Figures 6 and 7 were obtained from only a core part of the Izod test specimens. In the following sections, the lateral size of the stringlike phases in the SEM micrographs was estimated by that of the brighter portions, that is, PC-rich stringlike phases.

In the longitudinal micromorphology, the lateral size of the stringlike phases decreased from about 3.5 to 0.6 μm as the amount of the added PS–PAr block copolymer increased up to 3 wt %, as shown in Figure 6. Even if its amount surpassed 3 wt %, the lateral size seemed to suffer a further decrease, while the longitudinal length of the stringlike phases was unchanged irrespective of the amount of the PS–PAr block copolymer added.

On the other hand, the lateral micromorphology consisted of a cocontinuous phase with regu-

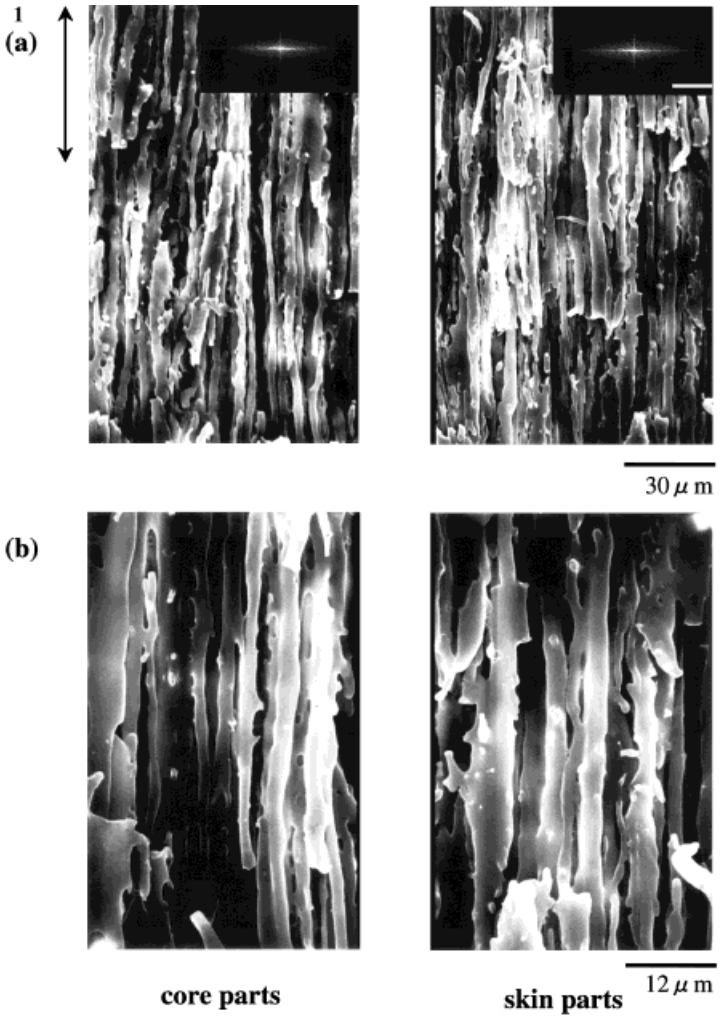

Figure 4 (1) Phase morphologies of 50/50 HIPS/PC blend obtained from the longitudinal section and their 2D-FFT patterns: (a) low and (b) high magnifications. The arrow indicates the flow direction. Bar in the 2D-FFT image corresponds to 6.88×10^2 (nm^{-1}). (2) Phase morphologies of 30/70 HIPS/PC blend obtained from the longitudinal section and their 2D-FFT patterns: (a) low and (b) high magnifications. The arrow indicates the flow direction. Bar in the 2D-FFT image corresponds to 6.88×10^2 (nm^{-1}).

lar spacing (Fig. 7). To discuss the regularity of this cocontinuous structure pinpointedly, Figure 8 shows a typical 2D-FFT pattern based on the SEM micrographs of Figure 7(a,d). The 2D-FFT patterns essentially showed a ring structure with a specific periodic wavelength, the so-called the spinodal ring.[47–49] This kind of 2D-FFT pattern indicates that these cocontinuous structures had a specific periodic distance, shown as Λ_c in Figure 7. This Λ_c value seemed almost equal to the lateral periodic distance of the stringlike phase (Λ_l) defined in Figure 6 for each sample. This is because all these continuous phases were originated from the interconnection or blanching among the stringlike phases. Its value also decreased from about 5 to 1.5 μm, with the increase in weight percent of the added PS–PAr block copolymer up to 3 wt %. When the amount of the PS–PAr block copolymer added exceeded 3 wt %, the Λ_c value suffered no more decrease.

Considering these experimental results, the PS–PAr block copolymer was found to successfully compatibilize HIPS/PC blends. With the addition of the PS–PAr block copolymer to the HIPS/PC blend system by 3–5 wt %, the lateral size of the stringlike phases could be reduced to about 1/3 times smaller than that of the simple blend system.

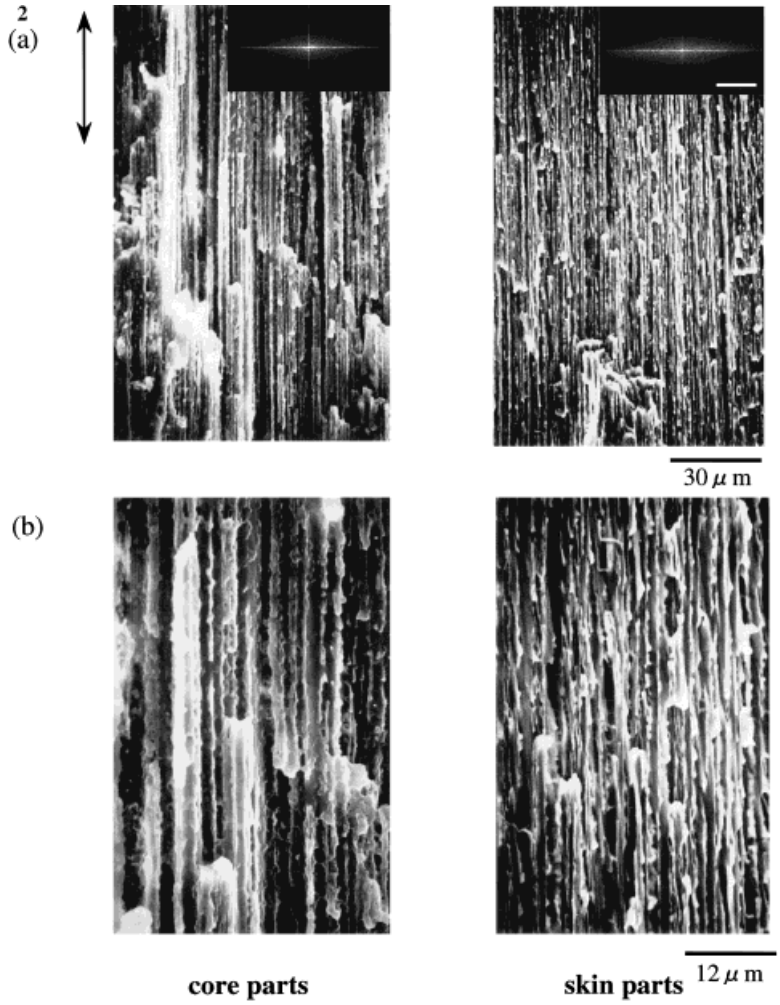

Figure 4 (Continued)

Effect of Shear Rate on Morphology Generation

The lateral size of the stringlike phases observed under a shear flow field was reported to decease with an increasing shear rate, and, furthermore, under a shear field exceeding the critical point, a flow-induced homogenization occurs.[41–45] To clarify the effect of the shear rate on the morphology generation, Figure 9 indicates the stringlike phases of the extruded blends of 50/50 HIPS/PC as a function of the average shear rate. The morphologies in Figure 9 were obtained from the pelletized specimens. The average shear rate during the extrusion process was varied from 225 to 900 s^{-1} according to the fed amount versus the shear rate curve in Figure 3. In these series of the extrusion experiments, the blends were compatibilized with 3 wt % of the PS–PAr block copolymer.

The lateral size of the string phases decreased from about 2.3 to 0.6 μm with an increasing shear rate from 225 to 680 s^{-1} (Fig. 9). When the shear rate reached 680 s^{-1} and above, the lateral size of the string phases seemed to converge to the same level. In this region of the shear rate, no kind of shear-induced homogenization ever occurred.

Mechanical Properties of HIPS/PC Blends

Tensile Properties

In Table II, the tensile properties of the HIPS, PC, and HIPS/PC blends are given. The experimental error bar in Table II shows the range of data excluding the maximum and minimum values. As shown in Table II, the tensile modulus and yield strength of the HIPS/PC blends were basically according to the addition rule of the amount of HIPC and PC, while the elongation of the HIPS/PC blends was almost equal to that of PC. There was little difference between uncompatibilized and compatibilized HIPS/PC blends.

In the HIPS/PC blends, HIPS- and PC-rich stringlike phases were essentially connected in the parallel direction to the flow, that is, the tensile direction. Thus, the parallel connection model of the respective HIPS and PC phases whose contribution ratio is determined by its blend composition could explain these tensile behaviors. In the parallel-connection model, the strain is commonly bore by both phases and stored energy at the yield point should be additional, whereas the value of the elongation at break should be dominated by the specific phase with superior ductility. As a result of this interpretation, the value of the modulus and yield stress should be according to the additional values of each component contribution. Also, the value of the elongation should be almost equal to that of PC. Judging from the good agreement between these estimations and the experimental data, it may be concluded that the tensile behaviors of the HIPS/PC blends can be reasonably well explained by the parallel-connection model of the HIPS and PC phases.

Energy-absorbing Properties of the HIPS/PC Blends

Figure 10(a) shows the Izod impact strength of the HIPS/PC blends. The uncompatibilized HIPS/PC blend showed a low Izod impact strength of 230 J/m at a composition of 50/50, while at a 30/70 composition, it showed a relatively high Izod impact strength of 470 J/m. Under the compatibilization condition using the PS–PAr block copolymer, the Izod impact strength increased monotonically as the weight percent of the added PS–PAr block copolymer increased up to 3 wt %, above which no further increase was observed up to 5 wt %. When compatibilized with a 3 or 5 wt % addition of the PS–PAr block copolymer, the HIPS/PC blend exhibited a higher than 1000 J/m Izod impact strength even at the composition of 50/50.

To correlate this energy-absorbing behavior of the HIPS/PC blends to their microphase morphology, Figure 10(b) shows the relationship between the lateral size of the PC-rich stringlike phase and the Izod impact strength. The Izod impact strength of the HIPS/PC blend increased as the lateral size of the stringlike phases decreased. Especially when the lateral size of the stringlike phase was smaller than about 1.0 μm, the Izod impact strength reached higher than 1000 J/m. These results indicate that the lateral size of the string phases is a dominant parameter in determining the energy-absorbing behavior of the HIPS/PC blends.

Effect of the Rubber Particle Size in HIPS on Energy-absorbing Properties of the HIPS/PC blends

To explore how the rubber particle size in HIPS affects the energy-absorbing properties of the HIPS/PC blends, a series of Izod impact strengths

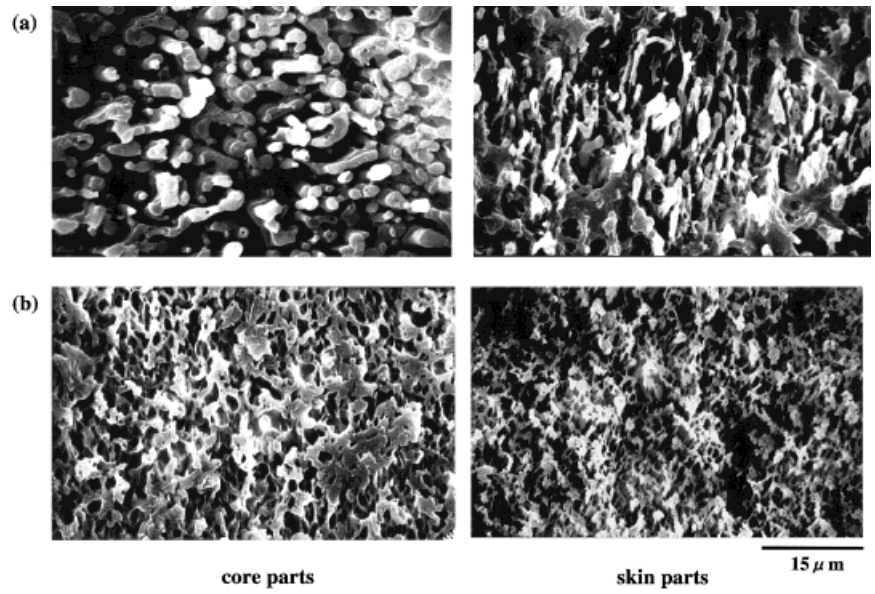

Figure 5 Phase morphologies of 50/50 and 30/70 HIPS/PC blends obtained from the lateral section: (a) 50/50 and (b) 30/70 blends at high magnification.

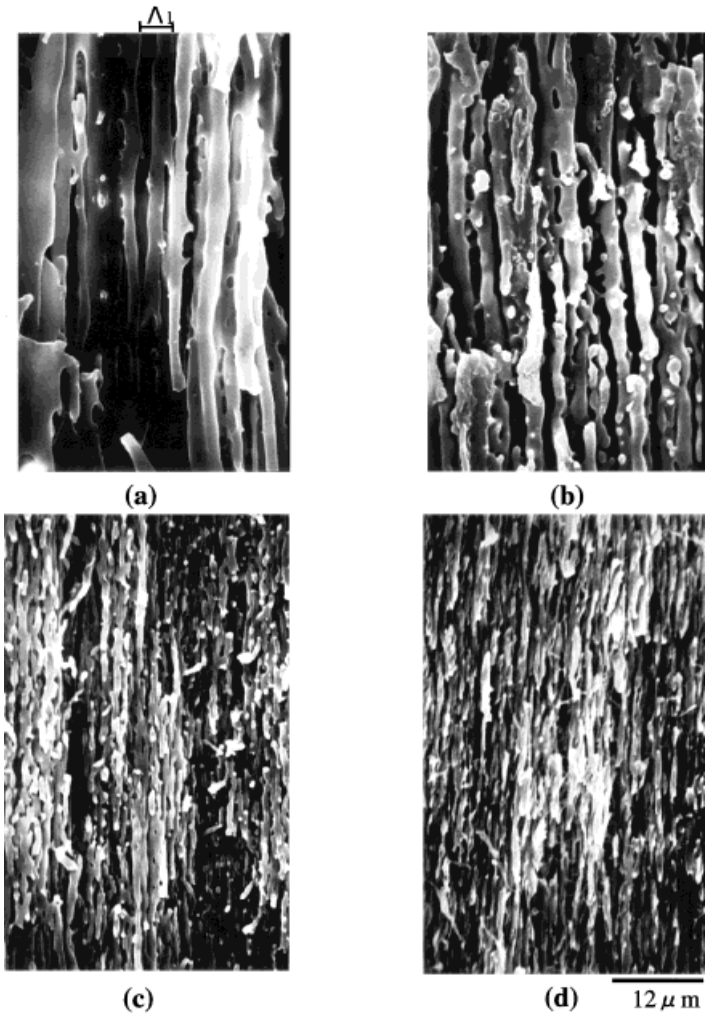

Figure 6 Phase morphologies of 50/50 HIPS/PC blends obtained from the longitudinal section, as a function of weight percent of the added PS–PAr block copolymer. The weight percents of the added PS–Par block copolymer are 0, 1, 3, and 5 for (a), (b), (c), and (d), respectively.

on the 50/50 HIPS/PC blends was carried out using HIPS with a different rubber particle size (H-650: rubber particle size is 3.5 μm on average). The results are shown in Figure 10(a). When HIPS with a 3.5-μm rubber particle was used, the 50/50 HIPS/PC blend exhibited almost the same Izod impact strength as that of the simply mixed blend, although it was compatibilized with a 3 wt % addition of the PS–PAr block copolymer. This result signifies that when HIPS with a relatively large rubber particle size was used, the PS–PAr block copolymer had no effect on the energy-absorbing properties of the HIPS/PC blend.

To clarify this postulation, a relationship between the stringlike phase size and the rubber particle size in HIPS was examined. Figure 11 shows TEM micrographs of the 50/50 HIPS/PC blends. Macroscopically, the morphology of these blends comprised two phases: One phase was the HIPS-rich phase containing rubber particles, and the other was the PC-rich phase. In the PC-rich phases, one can see several homo-PS domains as shown in Figure 11. These homo-PS originally belonged to HIPS. During the blend process, they were dissolved into the PC phases. The lateral size of the string phase was almost the same for both the HIPS- and PC-rich phases. There was a difference in the number of rubber particles contained in the HIPS-rich phase between the simply mixed and compatibilized HIPS/PC blends. In the simply mixed HIPS/PC blend, one can see several rubber particles in the lateral direction of the

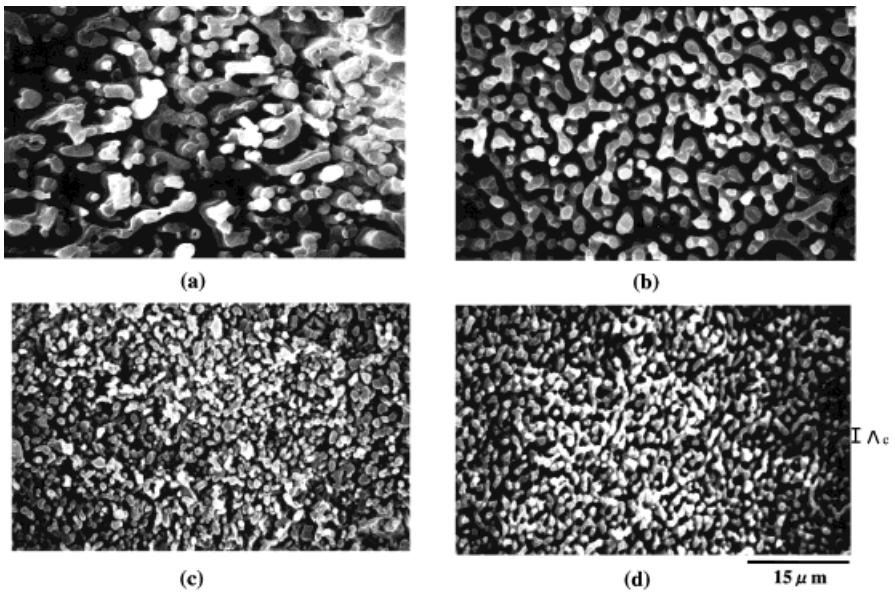

Figure 7 Phase morphologies of 50/50 HIPS/PC blends obtained from the lateral section, as a function of weight percent of the added PS–PAr block copolymer. The weight percents of the added PS–PAr block copolymer are 0, 1, 3, and 5 for (a), (b), (c), and (d), respectively.

HIPS-rich string as shown in Figure 11(a), while in the compatibilized blends, one can see almost one rubber particle there for both HIPS blends [Fig. 11(b,c)]. These results signify that the lateral size of the HIPS-rich phase could be reduced almost equal to the rubber particle size in HIPS by compatibilization with 3wt % of the PS–PAr block copolymer, regardless of the rubber particle size in HIPS. However, when the rubber particle in HIPS itself was large, the lateral size of the HIPS-rich string phases, which is almost equal to that of PC-rich phases, could not reach the high-impact region of Figure 10(b), even though they were reduced to the rubber particle size level. As a result, the HIPS/PC blends of Figure 11(c) showed a low Izod impact strength. These results indicate that the rubber particle size of HIPS is also a dominant factor in determining the energy-absorbing properties of the HIPS/PC blends. The rubber particle size in the used HIPS should be

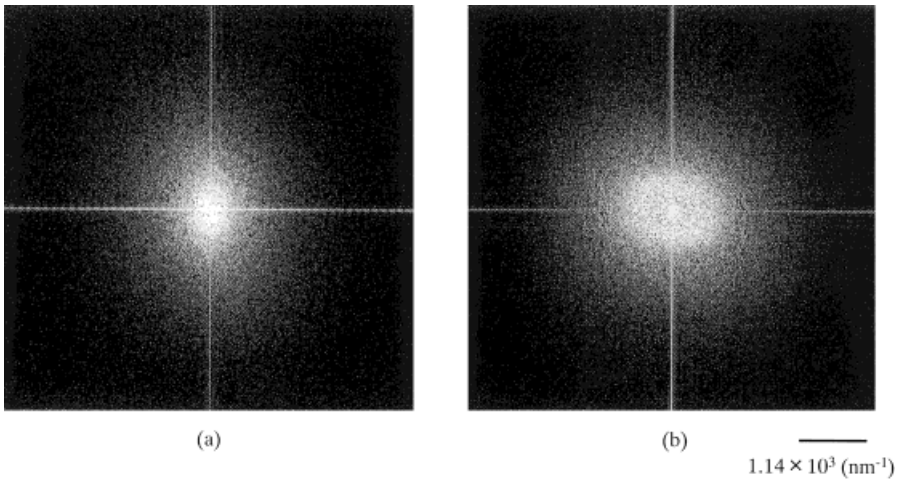

Figure 8 2D-FFT images calculated from SEM micrographs in Figure 6: (a) uncompatibilized and (b) compatibilized with 5 wt % of PS–PAr block copolymer.

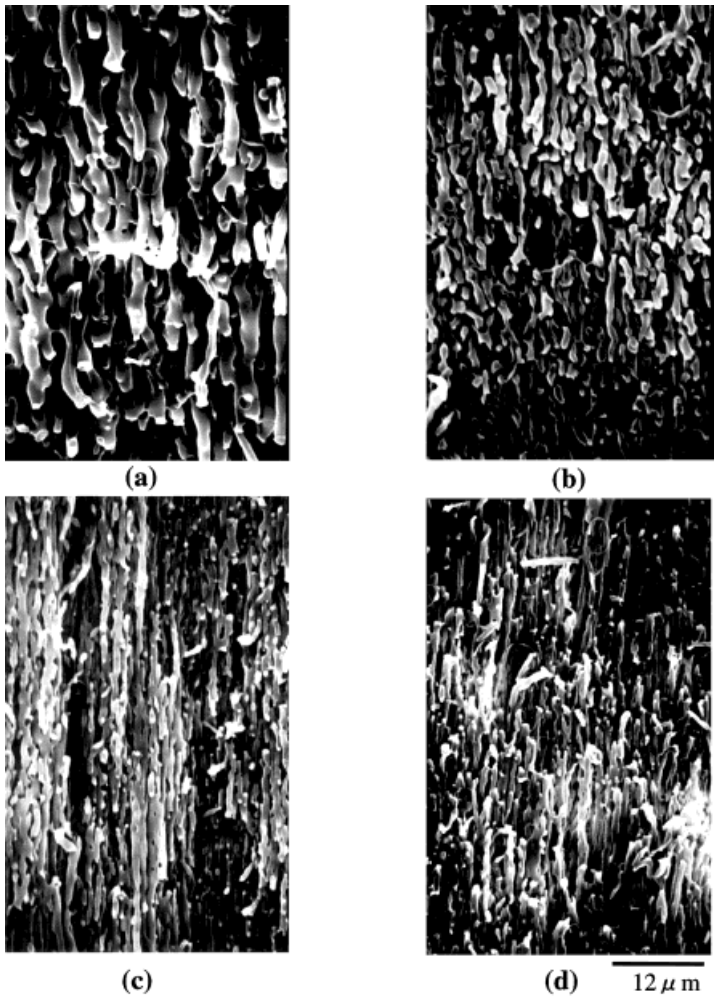

Figure 9 Stringlike phase of 50/50/3 HIPS/PC/PS–PAr block copolymer extruded blends as a function of average shear rate during the extrusion process. Average shear rate of (a), (b), (c), and (d) are 225, 450, 675, and 900 s^{-1}, respectively.

smaller than 1 μm to attain high-energy absorbency for the HIPS and PC blend system.

CONCLUSIONS

The phase morphology and mechanical properties of blends of HIPS with PC and the PS–PAr block copolymer were investigated. The PS–PAr block copolymer was found to successfully compatibilize the HIPS and PC blends. The main results and discussion are stipulated below:

1. The HIPS/PC blends form a cocontinuous structure induced by the flow during the extrusion or injection-molding process over a broad range of their composition from 50/50 through 30/70. These cocontinuous phases were characterized for their homogeneity. The micromorphology was affected by the molten flow and showed two different images dependent on the flow direction. One was the micromorphology in the longitudinal direction to the flow. The HIPS/PC blends exhibited stringlike phases highly elongated along the flow direction. These stringlike phases showed high continuity and regularity parallel and normal to the flow, respectively. Their longitudinal size along the flow was long enough to be longer than 180 μm, while their lateral size was shorter than 5 μm. The other was the morphology in the lateral direction to the flow. The HIPS/PC blends exhibited regular co-

Table II Tensile Properties of HIPS, PC, and HIPS/PC Blends

Polymer	Modulus (Gpa)	Yield Stress (Mpa)	Elogation at Break (%)
HIPS (XL-1)	1.72 ± 0.17	32.0 ± 0.17	27 ± 2
50/50-HIPS/PC	1.95 ± 0.10 (1.95)	44.4 ± 0.60 (47)	117 ± 4
50/50/3-HIPS/PC/PS–PAr	1.96 ± 0.09 (47)	44.7 ± 0.20 (47)	118 ± 2
30/70-HIPS/PC	2.10 ± 0.15 (2.04)	50.3 ± 0.40 (53)	111 ± 5
PC	2.18 ± 0.20	62.0 ± 0.50	115 ± 4

Nos. in parenthesis show the value predicted from the addition rule of each component.

continuous phases due to the interconnection or blanching among the stringlike phases. Their 2D-FFT images showed a so-called spinodal ring whose specific periodic distance almost equaled the lateral periodic distance of the stringlike phases in the longitudinal section.

2. The lateral size of the stringlike phases could be controlled both by the amount of the PS–PAr block copolymer added and by the shear rate during the extrusion process without changing their longitudinal size. The HIPS/PC blend compatibilized with 3 wt % of the PS–PAr block copolymer under an average shear rate of 675 s^{-1} showed a stringlike phase whose lateral size was reduced almost equal to the rubber particle size in HIPS. Even if the amount of the added PS–PAr block copolymer or the average shear rate surpassed 3 wt % and 675 s^{-1}, respectively, the lateral size of the stringlike phases seemed to suffer a further decrease.
3. The values of the tensile modulus and yield stress of the HIPS/PC blends were in accordance with the addition rule of each component contribution, while the values of the elongation at break were almost equal to that of PC. These kinds of mechanical properties can be reasonably well explained by the parallel connection model of each phase.
4. The Izod impact strength of the HIPS/PC blends strongly depends on the lateral size of the stringlike phases and the rubber particle size in HIPS. It was found that the size of the stringlike phases should be smaller than 1.0 μm to attain a higher than 1000 J/m Izod impact strength for this blend system.
5. Considering Conclusions 1, 2, and 4 comprehensively, the optimal conditions for attaining a high-energy absorbency in the HIPS/PC blend system could be determined as follows:

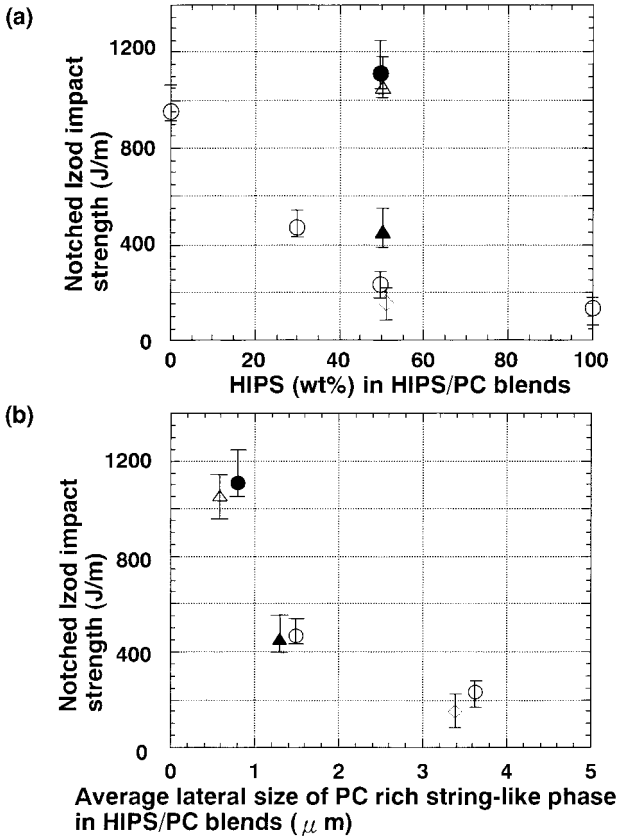

Figure 10 Notched Izod impact strength of HIPS/PC blends. Izod impact strength (a) as a function of HIPS weight percent in HIPS/PC blends and (b) as a function of lateral size of the PC-rich stringlike phase: (○) uncompatilized HIPS/PC; (▲, △, ●) HIPS/PC compatibilized with 1, 3, and 5 wt % of PS–PAr block copolymer, respectively. (◇) HIPS/PC/PS–PAr = 50/50/3, using HIPS with a 3.5-μm rubber particle.

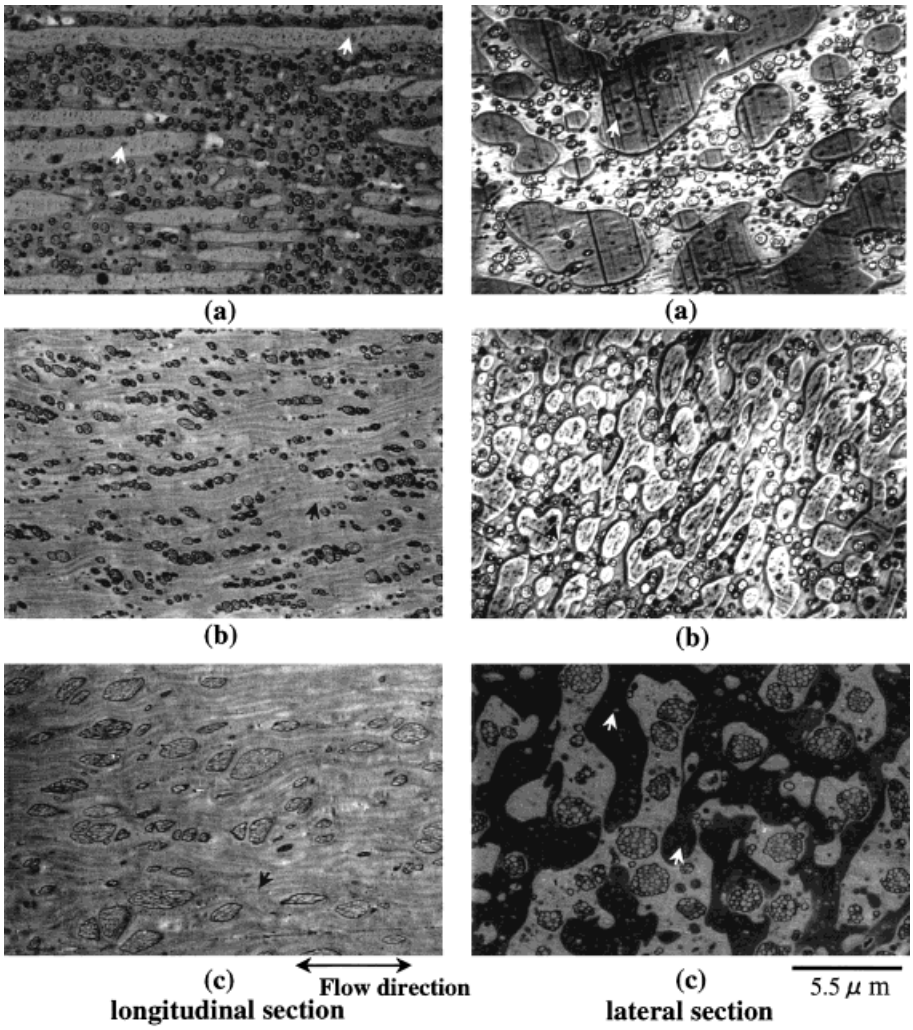

Figure 11 TEM micrographs of HIPS/PC blends: (a) 50/50 HIPS (0.6 μm)/PC blends; (b) 50/50/3 HIPS (0.6 μm)/PC/PS–PAr; (c) 50/50/3 HIPS (3.5 μm)/PC/PS–PAr blends. Nos. in parentheses show the rubber particle size in HIPS. Arrows in the micrographs indicate some examples of homo-PS domains dissolved into the PC phase.

(a) The PS–PAr block copolymer should be added as a compatibilizer at 3–5 wt %.
(b) HIPS, PC, and the PS–PAr block copolymer should be extruded at a shear rate higher than 675 s^{-1}.
(c) The rubber particle size in HIPS should be smaller than 1 μm.

The authors are grateful to Mr. S. Fujikawa of the Nippon Steel Chemical Co. for his technical assistance in taking the TEM micrographs. Also, the authors would like to thank Mr. K. Kometani and K. Ohwada of the Nippon Steel Chemical Co. for helping us in the experimental operation and in discussing the experimental results.

REFERENCES

1. Paul, D. R. Polymer Blends; Academic: New York, 1978; Vols. 1 and 2,.
2. Olabisi, O.; Robeson, L. M.; Shaw, M. T. Polymer–Polymer Miscibility; Academic: New York, 1979.
3. Akiyama, S.; Nishi, T.; Inoue, T. Polymer Blends; CMC: Tokyo, 1981.
4. Polymer Alloy, 2nd ed.; Kotaka, T., Ed.; Kagakudojin: Tokyo, 1993.
5. Utracki, L .A. Polymer Alloys and Blends; C. Hanser: Munich, 1990.
6. Inoue, T. Koubunsi 1996, 45, 447.
7. Paul, D. R.; Vision, C. E.; Locke, C. E. Polym Eng Sci 1972, 12, 157.

8. Coumans, W. J;. Heikins, D.; Sjoerdsma, S. D. Polymer 1980, 21, 103.
9. Trostyanskaya, E. B.; Zemskov, M. B.; Mikhasenok, O. Ya. Plast Massy 1983, 11, 28.
10. Fayt, R.; Jerome, R.; Teyssie, Ph. J Polym Sci Polym Lett Ed 1986, 24, 25.
11. Teyssie, Ph. Makromol Chem Macromol Symp 1988, 22, 83.
12. Anastsiadis, S. H.; Gancarz, I.; Koberstein, J. T. Macromolecules 1989, 22, 1489.
13. Heikens, D.; Barensten, W. M. Polymer 1977, 18, 70.
14. Brown, H. R. Macromolecules 1989, 22, 2859.
15. Shull, K. R.; Kramar, E. J. Macromolecules 1990, 23, 4769.
16. Nakayama, A.; Inoue, T.; Guegan, P.; Macosko, C. W. ACS Symposium Series 34; American Chemical Society: Washington, DC, 1993; p 840.
17. Brown, S. B. Annu Rev Mater Sci 1991, 21, 409.
18. Ide, F.; Kodama, T.; Hasegawa, A. Koubunsikagaku 1972, 29, 259.
19. Hobbes, S. Y.; Dekkers, M. E. J. J Mater Sci 1989, 24, 1316.
20. Carrot, C.; Guillet, J.; May, J. F. Plast Rubb Compos Process Appl 1991, 19, 61.
21. Majumdar, B.; Keskkula, H.; Paul, D. R. Polymer 1994, 35, 3165.
22. Majumdar, B.; Keskkula, H.; Paul, D. R. Polymer 1994, 35, 4263.
23. Majumdar, B.; Keskkula, H.; Paul, D. R. Polymer 1994, 35, 5468.
24. Ohishi, H.; Kimura, M. Nippon Steel Technical Report, 1993; Vol. 53, p 39.
25. Ohishi, H.; Ohwaki, T.; Nishi, T. J. Polym Sci Part A Polym Chem Ed 1998, 36, 2839.
26. Ohishi, H.; Nishi, T. Polym Sci Part A Polym Chem Ed 2000, 38, 288.
27. Ohishi, H.; Kishimoto, S.; Nishi, T. J. Appl Polym Sci 2000, 78, 953.
28. Ohishi, H.; Kishimoto, S.; Ikehara, T.; Nishi, T. J Polym Sci Part B Polym Phys Ed 2000, 38, 127.
29. Ohishi, H.; Ikehara, T.; Nishi, T. J Appl Polym Sci, to appear.
30. Kunori, T.; Geil, P. H. J Macromol Sci Phys B 1980, 18, 93.
31. Eastmond, G. C.; Haraguchi, K. Polymer 1983, 24, 1171.
32. Rundin, A.; Brathwaite, N. E. Polym Eng Sci 1984, 24, 1312.
33. Kim, W. N.; Burns, C. M. J Appl Polym Sci 1987, 34, 945.
34. Kim, W. N.; Burns, C. M. J Appl Polym Sci 1990, 41, 1575.
35. Mckay, I. D. J Appl Polym Sci 1991, 42, 281.
36. Kim, C. K.; Paul, D. R. Macromolecules 1992, 25, 3097.
37. Kim, C. K.; Paul, D. R. Polymer 1992, 33, 4941.
38. Sakellariou, P.; Eastmond, G. C Polymer 1993, 34, 3037.
39. Nishi, T.; Suzuki, T.; Tanaka, H.; Hayashi, T. Makromol Chem Macromol Symp 1991, 51, 29.
40. Kammer, H. W.; Kummerloewe, C.; Kressler, J.; Meilor, J. P. Polymer 1991, 32, 1488.
41. Wolf, B. A. Makromol Chem Rapid Commun 1980, 1, 231.
42. Takebe, T.; Fujioka, K.; Sawaoka, R.; Hashimoto, T. J Chem Phys 1990, 93, 5271.
43. Fujioka, K.; Takebe, T.; Hashimoto, T. J Chem Phys 1993, 98, 717.
44. Kume, T.; Asakawa, K.; Moses, E.; Mastuzaka, K.; Hashimoto, T. Acta Polym 1995, 46, 79.
45. Hashimoto, T.; Matsuzaka, K.; Moses, E.; Onuki, A. Phys Rev Lett 1995, 74, 126.
46. Mondragon, I.; Cortazar, M.; Guzman, G. M. Makromol Chem 1983, 184, 1741.
47. Synder, H. L.; Meakin, P.; Reich, S. Macromolecules 1983, 16, 757.
48. Hashimoto, T.; Kumaki, J.; Kawai, H. Macromolecules 1983, 16, 641.
49. Tanaka, H.; Hayashi, T.; Nishi, T. J Appl Phys 1986, 59, 3627.